AGU ADVANCING EARTH AND SPACE SCIENCE

JGR Atmospheres

RESEARCH ARTICLE
10.1029/2019JD032058

Potential Effect of Halogens on Atmospheric Oxidation and Air Quality in China

Qinyi Li[1], **Alba Badia**[1,2], **Tao Wang**[3], **Golam Sarwar**[4], **Xiao Fu**[3], **Li Zhang**[5,6,7], **Qiang Zhang**[8], **Jimmy Fung**[9], **Carlos A. Cuevas**[1], **Shanshan Wang**[10], **Bin Zhou**[10], and **Alfonso Saiz-Lopez**[1,10]

[1]Department of Atmospheric Chemistry and Climate, Institute of Physical Chemistry Rocasolano, CSIC, Madrid, Spain, [2]Now at Institute of Environmental Science and Technology (ICTA), Universitat Autònoma de Barcelona (UAB), Barcelona, Spain, [3]Department of Civil and Environmental Engineering, The Hong Kong Polytechnic University, Hong Kong, China, [4]National Exposure Research Laboratory, Environmental Protection Agency, Research Triangle Park, NC, USA, [5]Atmospheric and Oceanic Sciences, Princeton University, Princeton, NJ, USA, [6]Geophysical Fluid Dynamics Laboratory, National Oceanic and Atmospheric Administration, Princeton, NJ, USA, [7]Now at Department of Meteorology and Atmospheric Science, The Pennsylvania State University, University Park, PA, USA, [8]Department of Earth System Science, Tsinghua University, Beijing, China, [9]Division of Environment and Sustainability, Hong Kong University of Science and Technology, Hong Kong, China, [10]Department of Environmental Science and Engineering, Fudan University, Shanghai, China

Key Points:
- First assessment of halogen impact on the overall atmospheric oxidation over Chin
- Halogens result in enhanced oxidation throughout the year in polluted regions in China
- Large spatio-temporal heterogeneity of the halogen-mediated effect on oxidation capacity, which can be explained by the Asian monsoon, the location and intensity of halogen sources, and the ozone formation regime
- First regional model evaluation of halogen impact on air quality in China

Supporting Information:
- Supporting Information S1

Correspondence to:
A. Saiz-Lopez,
a.saiz@csic.es

Citation:
Li, Q., Badia, A., Wang, T., Sarwar, G., Fu, X., Zhang, L., et al. (2020). Potential effect of halogens on atmospheric oxidation and air quality in china. *Journal of Geophysical Research: Atmospheres*, *125*, e2019JD032058. https://doi.org/10.1029/2019JD032058

Received 14 NOV 2019
Accepted 7 MAR 2020
Accepted article online 19 APR 2020

Abstract Air pollution has been a hazard in China over recent decades threatening the health of half a billion people. Much effort has been devoted to mitigating air pollution in China leading to a significant reduction in primary pollutants emissions from 2013 to 2017, while a continuously worsening trend of surface ozone (O_3, a secondary pollutant and greenhouse gas) was observed over the same period. Atmospheric oxidation, dominated by daytime reactions involving hydroxyl radicals (OH), is the critical process to convert freshly-emitted compounds into secondary pollutants, and is underestimated in current models of China's air pollution. Halogens (chlorine, bromine, and iodine) are known to profoundly influence oxidation chemistry in the marine environment; however, their impact on atmospheric oxidation and air pollution in China is unknown. In the present study, we report for the first time that halogens substantially enhance the total atmospheric oxidation capacity in polluted areas of China, typically 10% to 20% (up to 87% in winter) and mainly by significantly increasing OH level. The enhanced oxidation along the coast is driven by oceanic emissions, and that over the inland areas by anthropogenic emission. The extent and seasonality of halogen impact are largely explained by the dynamics of Asian monsoon, location and intensity of halogen emissions, and O_3 formation regime. The omission of halogen emissions and chemistry may lead to significant errors in historical re-assessments and future projections of the evolution of atmospheric oxidation in polluted regions.

1. Introduction

Degraded air quality has become one of the dominant worldwide causes of mortality, with 3.3 million premature deaths each year in the world and 1.3 million in China (Lelieveld et al., 2015). The level of pollutants in the atmosphere is determined by primary pollutants emission, meteorological conditions, and the conversion of primary emissions to secondary pollution by atmospheric oxidation (Seinfeld & Pandis, 2006). Much attention has been paid to the first two factors (Fu et al., 2019). In 2013, China launched an aggressive policy (Air Pollution Prevention and Control Action Plan) that led to a significant decrease in the primary pollutants emission; for instance, nitrogen oxides (NO_x), sulfur dioxide (SO_2), and primary fine particulate matter ($PM_{2.5}$) decreased by 21%, 59%, and 33%, respectively, from 2013 to 2017 (Zheng et al., 2018). Meteorological conditions mainly induce diurnal and seasonal variations on air pollution and have less effect on the year-to-year variability. The level of surface O_3, a secondary pollutant, experienced a gradual increase of 1 to 3 ppbv (parts per billion in volume) per year from 2013 to 2017 in the megacity clusters in China and the sharp decrease (~40%) of ambient level of $PM_{2.5}$ in these regions was proposed to be the main cause (Li, Jacob, et al., 2019). The formulation of control policies for secondary pollutants demands a comprehensive understanding of atmospheric oxidation (Monks et al., 2015; Wang, Xue, Brimblecombe et al., 2017).

However, mechanisms in current models underestimate atmospheric oxidation in polluted environments in China due to the lack of sufficient knowledge in the production and destruction mechanisms of the main atmospheric oxidants (Lu et al., 2018; Tan et al., 2019), OH, O_3, NO_3 (nitrate radical), and Cl.

Halogen chemistry is well known for destroying stratospheric O_3 (Solomon, 1999). In the troposphere, Reactive Halogen Species (RHS, halogen species with a lifetime shorter than 180 days), emitted from both anthropogenic and natural sources, have been reported to oxidize volatile organic compounds (VOC) to increase the production of OH, the hydroperoxyl radical (HO_2), and O_3 (R1-R5); to directly destroy O_3 (R6); to transform the partitioning between OH and HO_2 (R7-R8); to change the partitioning of NO and NO_2 (R9); and to indirectly destroy O_3 by providing a sink for NO_2 (R10-R11) (Saiz-Lopez & von Glasow, 2012; Simpson et al., 2015).

$$\mathrm{Cl + VOC \rightarrow RO_2 + HCl} \tag{R1}$$

$$\mathrm{RO_2 + NO \rightarrow NO_2 + HO_2} \tag{R2}$$

$$\mathrm{HO_2 + NO \rightarrow NO_2 + OH} \tag{R3}$$

$$\mathrm{NO_2 + hv \rightarrow NO + O\left(^3P\right)} \tag{R4}$$

$$\mathrm{O\left(^3P\right) + O_2 \rightarrow O_3} \tag{R5}$$

$$\mathrm{X + O_3 \rightarrow XO \; X = Cl, Br, and\ I} \tag{R6}$$

$$\mathrm{XO + HO_2 \rightarrow HOX} \tag{R7}$$

$$\mathrm{HOX + hv \rightarrow X + OH} \tag{R8}$$

$$\mathrm{XO + NO \rightarrow X + NO_2} \tag{R9}$$

$$\mathrm{XO + NO_2 \rightarrow XONO_2} \tag{R10}$$

$$\mathrm{XONO_2 + H_2O(1) \rightarrow HOX + HNO_3(1)} \tag{R11}$$

Several large-scale (global and hemispheric) modeling studies have been reported on the effect of halogens in the troposphere. Sarwar et al. (2014) included the $ClNO_2$ production from N_2O_5 heterogeneous uptake in the Community Multiscale Air Quality (CMAQ) model and evaluated the effect of this process on O_3 in the northern hemisphere. von Glasow et al. (2004) incorporated relevant reactions of bromine species in a global model, MATCH-MPIC, and explored the influence of bromine on O_3 and DMS in the marine boundary layer. Ordóñez et al. (2012), Fernandez et al. (2014), and Saiz-Lopez et al. (2014) implemented the sources and chemistry of chlorine, bromine, and iodine, in the CAM-Chem global model, and revealed the important role of their combined chemistries in the troposphere. Sarwar et al. (2015) further developed CMAQ to examine the influence of the bromine and iodine chemistry and sources on surface O_3 in the northern hemisphere. Hossaini et al. (2016) updated a global model, TOMCAT, with comprehensive chemistry and sources of chlorine species, and reported the burden of chlorine and its influence on methane (CH_4) in the troposphere. Sherwen et al. (2016) added the chemistry of chlorine, bromine, and iodine in the GEOS-Chem global model, and reported their role in the troposphere. Stone et al. (2018) adopted the GEOS-Chem model and evaluated the impact of bromine and iodine chemistry on OH and HO_2 in the troposphere. Wang et al. (2019) refined the representation of chlorine chemistry in the GEOS-Chem model and estimated the impact of chlorine on the compositions in troposphere.

Only modeling studies on the effect of chlorine have been conducted in China. Li et al. (2016) implemented the production of $ClNO_2$ from the heterogeneous uptake of N_2O_5 on chloride-containing aerosol in the Weather Research and Forecasting model coupled with Chemistry (WRF-Chem) and evaluated the chlorine chemistry effect on surface O_3 and reactive nitrogen in winter in China. Zhang et al. (2017) updated the chlorine chemistry in WRF-Chem and estimated its impact on surface O_3 in summer in China. Qiu et al. (2019a, 2019b) incorporated several heterogeneous reactions of chlorine in the CMAQ model and reported the effect of these reactions on nitrate, O_3, and OH radical. However, no regional modeling studies

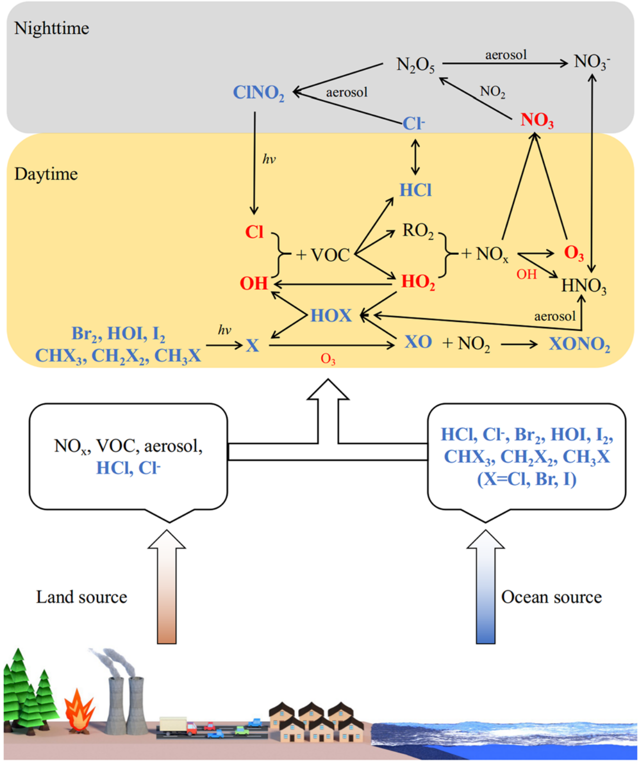

Figure 1. Schematic of the impact of halogen on atmospheric oxidation. Cl and OH radicals initiate the oxidation of VOCs (emitted from anthropogenic and biogenic sources), which produces HO_2 and RO_2. HO_2 and RO_2 then form surface O_3 with the presence of NO_x (from anthropogenic sources). O_3 reacts with NO_2 at night to form NO_3, the nighttime radical leading to the formation of $ClNO_2$, which photolyses to release Cl atoms. Oceanic emission of (both organic and inorganic) halogen species with the contribution from anthropogenic pollutants (O_3, HNO_3, etc.) releases halogen atoms (X = Cl, Br, I) which destructs O_3, forms XO, recycles X, and transforms HO_2 to OH.

of the overall influence of halogens on atmospheric oxidation and air pollution has been reported in China, one of the most polluted regions in the world.

In this study, we present an in-depth analysis employing a widely used regional air quality model, WRF-Chem (Grell et al., 2005), implemented with state-of-the-art halogen chemistry and sources (Badia et al., 2019). We estimate the abundance of RHS and isolate their impact (by conducting sensitivity tests with and without RHS) on O_3 and atmospheric oxidation in four dimensions (temporal and the three spatial dimensions), which has more implications for broader temporal periods and spatial extent compared with measurements and observation-constrained box modeling. Applying a regional chemical transport model (CTM) also helps to reproduce finer and more realistic emissions and meteorological processes compared with a global model. We find that halogens exert a large control on the regulation of the individual oxidants and the overall atmospheric oxidation in China.

2. Materials and Methods

2.1. WRF-Chem Model

The WRF-Chem model is a widely used regional CTM; version 3.7.1 was used in the present study. The halogen chemistry implemented in WRF-Chem is described in Badia et al. (2019), also sketched in Figure 1. In particular, Badia et al. (2019) followed the approach used by other models, e.g., TOMCAT (Hossaini et al., 2016), CAM-Chem (Ordóñez et al., 2012) and GU–WRF/Chem (Karamchandani et al., 2012), to implement heterogeneous reactions of halogens (reactions shown in Table S1). In this approach, the heterogeneous chemistry is assumed to take place between a gas-phase species and an adsorbed species with an uptake coefficient used to calculate first-order rate constants for heterogeneous loss of the gas-phase species. Note that the pH value of the aerosol particles is calculated in the aerosol module (MOSAIC) for each size bin (Zaveri et al., 2008).

The WRF-Chem model has included the general source and loss of atmospheric oxidants and their precursors, namely (1) the production of OH from heterogeneous formation of HONO on aerosols and ground surfaces (following Zhang et al., 2017) and the photolysis of O_3, H_2O_2, and oxygenated VOC; (2) the production of HO_2 and O_3 after the initial OH reactions with VOC; (3) the formation of NO_3 from NO_2 and O_3; and (4) the activation of Cl atoms from the heterogeneous uptake of N_2O_5 on chloride-containing aerosol surfaces.

2.2. Data

Surface O_3 measurement data were obtained from the Ministry of Ecology and Environment in China (http://www.mee.gov.cn/hjzl/dqhj/qgkqzlssfb/) for the evaluation of WRF-Chem simulation (section 2.3 and 3.2). Meteorological datasets (ds083.2, ds351.0, and ds461.0) were obtained from the NCEP for the simulation of meteorology. Initial and boundary data for all simulations were obtained from a global simulation without halogens in CAM-Chem (Cuevas et al., 2018), because the focus of the present work is to evaluate the potential influence of the halogens emitted within the domain on the oxidation capacity. We used the Multi-resolution Emission Inventory in China (MEIC) (www.meicmodel.org) for the routine species (NO_x, SO_2, CO, VOC, NH_3, $PM_{2.5}$, PM_{10}). The preparation (temporal and vertical allocation) of raw emission data for the use in WRF-Chem follows Li et al. (2016). A daily fire emission inventory, the Fire Inventory from NCAR (FINN) (Wiedinmyer et al., 2011), was also used in the present study.

For the sources of halogens (Figure 2), oceanic halogen emissions were calculated online following Badia et al. (2019). A list of sources of reactive halogens considered in this study are: an oceanic source of

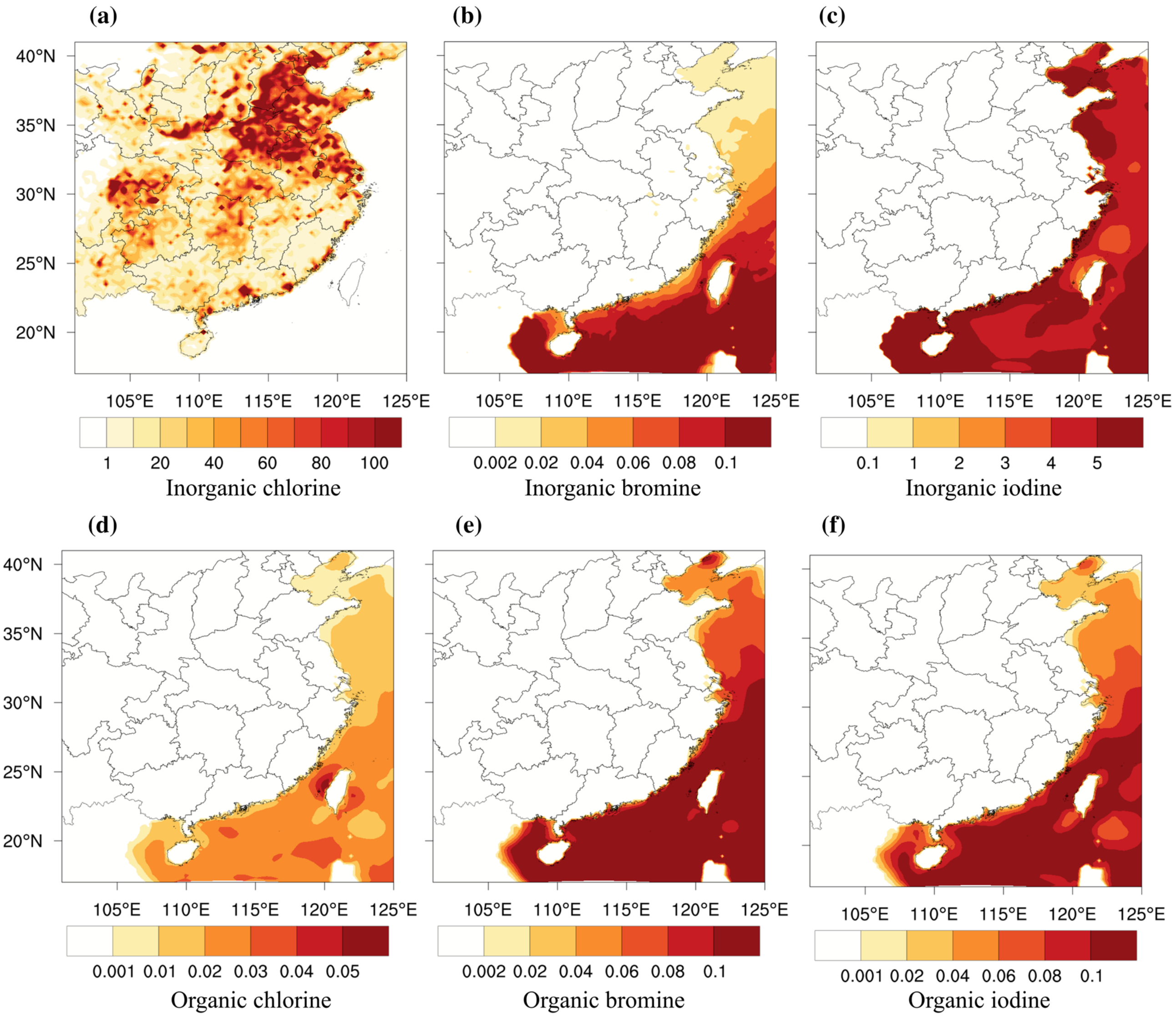

Figure 2. Annual average emissions (multiplied by 10^{13}) of Cl, Br, and I species (kg m^{-2} s^{-1}).

organic halogens ($CHBrCl_2$, CH_2BrCl, $CHBr_2Cl$, $CHBr_3$, CH_2Br_2, CH_2ICl, CH_2IBr, CH_2I_2, and CH_3I), debromination (Br_2, IBr), and inorganic I from the ocean (HOI and I_2). A two-layer model (Liss & Slater, 1974) is used to calculate the organic halogens air–sea fluxes online. An important source of reactive inorganic bromine in the troposphere is the release of bromine species from sea-salt aerosols into the gas-phase, also known as debromination. The oceanic emission of inorganic iodine (HOI and I_2) follows the deposition of O_3 to the surface ocean and reaction with iodide (I-) (Carpenter et al., 2013).

An up-to-date and high-resolution anthropogenic inventory of hydrogen chloride (HCl) and fine particulate Cl- emissions (from coal burning, biomass burning, and municipal solid waste burning) for China was used (Fu et al., 2018), which was developed based on a bottom-up method with detailed local data (e.g. Cl content in coal, point source information, etc.) and county-level activity data. The role of anthropogenic chlorine emissions on a global scale is still under debate (Hossaini et al., 2016; Wang et al., 2019), however, the observations in China have revealed the ubiquitous existence of chlorine species that originated from anthropogenic sources (e.g., Tham et al., 2016; Wang, Wang, Tham et al., 2017; Yang et al., 2018). Therefore, it is necessary to include the anthropogenic chlorine emissions in evaluating the overall impact of halogen species on atmospheric oxidation and air quality in China.

Table 1
Simulation Cases Setup

Cases	Anthropogenic chlorine emission	Oceanic halogen emission	Chlorine chemistry	Bromine chemistry	Iodine chemistry
BASE	No	No	No	No	No
HAL	Yes	Yes	Yes	Yes	Yes
OCN	No	Yes	Yes	Yes	Yes
CHL	Yes	Yes	Yes	No	No
CHL + BRM	Yes	Yes	Yes	Yes	No

2.3. Simulation Setup

The domain of WRF-Chem simulation was selected to cover the main city-clusters in China (Figure S1a and S1b, the red boxes represent regions of northern and southern China). We used a spatial resolution of 27 km and 30 vertical layers with the surface layer ~20 m above ground level. The simulation period included the entire year of 2018. We ran the WRF-Chem model for each month of 2018 with an extra spin-up period of 10 days. In the current study, we divided the months into four seasons: spring includes March, April, and May; summer is June, July, and August; autumn is September, October, and November; and winter is January, February, and December. RRTMG is used as the shortwave and longwave radiation scheme (Iacono et al., 2008), the Noah scheme as the Land-surface model (Chen & Dudhia, 2001), the Morrison double-moment scheme as the Microphysics option (Morrison et al., 2009), the Mellor-Yamada-Janjic scheme for the planetary boundary layer (PBL) (Janjić, 1994), MOZART as the gas phase chemistry (Emmons et al., 2010), MOSAIC for the aerosol chemistry (Zaveri et al., 2008), and FTUV for the photolysis (Tie et al., 2003).

Five sets of simulations were conducted in the present study (Table 1), BASE, OCN, CHL, CHL + BRM, and HAL. Changes in atmospheric compositions between BASE and HAL represent the impact of the overall halogen sources and chemistry; those between the BASE and OCN scenarios represent the impact of oceanic emissions of RHS; difference between OCN and HAL shows the impact of anthropogenic chlorine emissions; CHL minus BASE isolates the impact of chlorine chemistry; changes from CHL to CHL + BRM are the effect of bromine chemistry; and those from CHL + BRM to HAL are the effect of iodine chemistry.

The model performance of BASE and HAL cases was evaluated using the ambient measurement of O_3, CO, and NO_2 (Figure S2), and the results suggest that both cases were able to simulate the general distribution of these routine air pollutants and HAL case appeared to improve the performance in hundreds sites.

2.4. Atmospheric oxidation capacity calculation

To quantify the effects of halogens on the overall oxidation in the atmosphere, we adopt the concept of atmospheric oxidation capacity (AOC, $\# \ cm^{-3} \ s^{-1}$) (Xue et al., 2015). AOC is defined in Equation 1. AOC is a unified metric (combining all oxidants, OH, O_3, NO_3, and Cl, their reactants, and rates of reactions) that represents the quantity of carbon oxidized in the atmosphere within a time period. AOC is more universal compared with the level of oxidants, the production rates of oxidants, the lifetime of VOC species, and the reactivity of oxidants (multiplying the reaction rates and the reactant level).

$$AOC = \sum_{i=1}^{m} \left([OX_i] \times \sum_{j=1}^{n} \left(a_j \times [C_j] \times k_{i,j} \right) \right) \tag{1}$$

In Equation 1, m and n denote the number of oxidants (4) and the number of reactant (VOC and CO) species (61), $[OX_i]$ is the concentration of oxidant i ($\# \ cm^{-3}$), a_j is the number of carbon atoms in reactant j, $[C_j]$ is the concentration of reactant j ($\# \ cm^{-3}$), and $k_{i,j}$ is the reaction rate constant of oxidant i and reactant j ($cm^3 \ \#^{-1} \ s^{-1}$). The reactions of oxidants and reactants are included in the Table S2.

For the reactants, we only included the organic species (all VOC species) and CO, in the calculation of AOC. We did not include NO_x and SO_2, because the reactions of NO_x with oxidants are generally reversible, e.g., the balance of NO-NO_2-O_3, and NO_2-O_3-NO_3-N_2O_5. For the oxidants, we included all the main oxidants (OH, O_3, NO_3, and Cl) in our model that react with the above-listed reactants, although HO_2 and Br might also contribute a small fraction to the AOC in the real atmosphere. The reaction rates, air temperature, and air density are from the model output.

3. Results and Discussion

3.1. Simulated Levels of Reactive Halogen Species

The simulated spatial distribution of the reactive halogen species in China is shown in Figure 3. The WRF-Chem model (HAL scenario) simulated a significant amount of inorganic chlorine species excluding HCl ($Cl_y = ClNO_3 + ClNO_2 + 2Cl_2 + HOCl + ClO + Cl + BrCl + ICl$) loading (> 600 parts per trillion in volume, pptv) in China especially over the polluted region, which results from the large anthropogenic chlorine emission (Fu et al., 2018). Cl_y loading peaks in winter and has a lowest level in summer, primarily due to the higher consumption of coal and lower temperature in winter facilitating the activation of chlorine from chloride aerosol.

This work also estimates a non-negligible level (>0.5 pptv) of inorganic bromine ($Br_y = HBr + BrNO_3 + BrNO_2 + 2Br_2 + HOBr + BrO + Br + BrCl + IBr$) and iodine ($I_y = HI + INO_3 + INO_2 + INO + 2I_2 + HOI + 2I_2O_4 + 2I_2O_3 + 2I_2O_2 + IO + I + ICl + IBr$) along the coast and a level of a few pptv over the ocean outside of the coast. The seasonal variation of Br_y and I_y appear to be higher in summer and lower in winter, partly because the levels of oxidants are higher in summer (Section 3.2) leading to more efficient activation of bromine and iodine from sea-salt aerosol. Also, the meteorology in China is governed by the Asian monsoon with southeasterly winds dominating in summer and northerly winds during winter (Figure S1c and S1d). The summer monsoon moves the oceanic emission of RHS into the land, whereas the winter monsoon blows the air from the land to the ocean and thus prevents the ocean-emitted RHS from entering Mainland China.

The simulation of halogen species is evaluated using the available measurements in the region (Table S3). Tham et al. (2014) reported the first field measurement of $ClNO_2$ in China and they reported an average value of 148.0 pptv in Aug, 2012, while WRF-Chem simulated 25 pptv in Aug, 2018 (with the monthly average of 14 to 131 pptv in the year of 2018). Wang et al. (2016) conducted a field campaign at a mountain site (Tai Mo Shan in Hong Kong) in winter 2013 and reported an average of 74.6 pptv, and WRF-Chem predicted an average of 146 pptv in Nov and Dec, 2018 (22–183 pptv, the numbers shown in brackets in this paragraph are the ranges of monthly average results). Tham et al. (2016), Wang, Wang, Tham, et al. (2017), and Wang et al. (2017) carried out a series of campaigns in three different sites (suburban, mountain, and urban sites, respectively) in the northern part of China, and found averages of 159.5, 30.4, and 94.0 pptv, respectively. WRF-Chem model estimated averages of 271 (206–754), 261 (202–895), and 494 (208–906) pptv, respectively. Yun et al. (2018) reported the currently highest $ClNO_2$ level, 8300 pptv (1 min average), measured in Heshan (a suburban site) during an extremely polluted episode, and the campaign average $ClNO_2$ is 1100 pptv, while WRF-Chem predicted an average of 293 (36–293) pptv. Zhou et al. (2018) measured an average of 174.3 pptv of $ClNO_2$ in Beijing in Jun, 2017 and WRF-Chem estimated 75 (75–283) pptv. Yang et al. (2018) compiled the available observation datasets of chloride aerosol in China from the year of 1997 to 2012. They found ubiquitous presence of particulate chloride in $PM_{2.5}$ across China and the campaign average concentration of fine chloride aerosol ranged between 0.11 $\mu g\ m^{-3}$ (in a background site, Tung Chung, in Summer) to 8.98 $\mu g\ m^{-3}$ (in an urban site, Ji'nan, in winter). WRF-Chem simulation estimated a similar range of fine chloride aerosol in China, from lower than 1 $\mu g\ m^{-3}$ (seasonal average of daily-maximum) in clean environment to more than 5 $\mu g\ m^{-3}$ in polluted areas. Overall, WRF-Chem model generally reproduced the level of $ClNO_2$ and chloride aerosol in China. The causes of the uncertainty include: (1) the uncertainty of parametrization for N_2O_5 heterogeneous uptake and the $ClNO_2$ yield (e.g. McDuffie et al., 2018; Tham et al., 2018); (2) the limitation of grid size might also affect the ability to reproduce the measured level of $ClNO_2$, for instance, artificially diluting the emission of NO and promoting the formation of NO_3 and N_2O_5 while leads to $ClNO_2$ production; (3) the limitation of grid size to fully reproduce the complex terrain characterization; (4) the lack of ability of WRF-Chem model to reproduce the extreme meteorological and chemical condition; (5) the uncertainty in the emissions, including the routine air pollutants, anthropogenic chlorine, and oceanic halogens; (6) the uncertainty in the aerosol treatment (e.g., number of the bins) which influences the

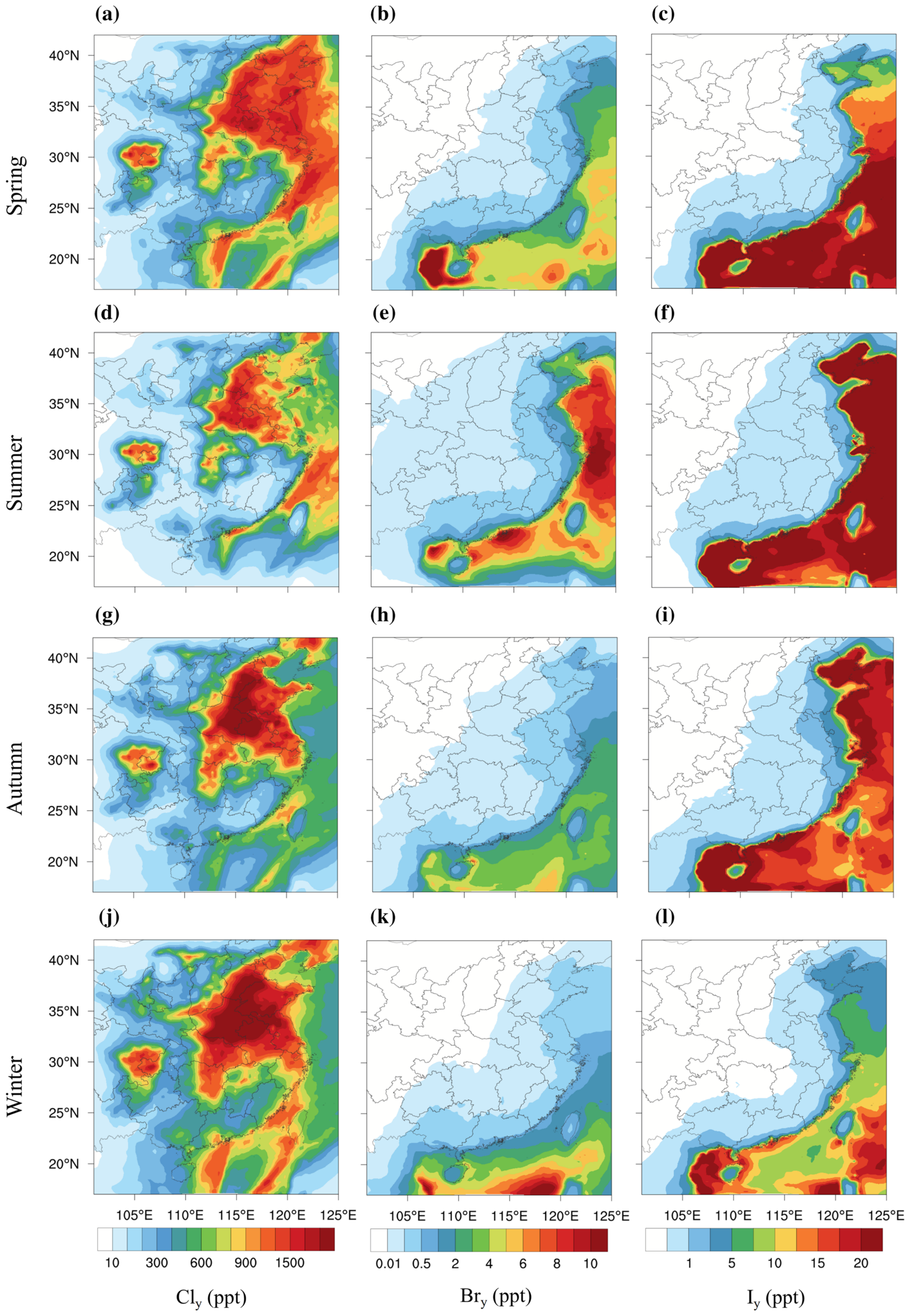

Figure 3. Seasonal averages of daily-maximum of Cl_y, Br_y, and I_y (pptv) at the surface in the HAL scenario.

calculation of surface area and therefore the rate of heterogeneous reactions; and (7) other heterogeneous reactions of chlorine species that are not included in the current study (e.g., Qiu et al., 2019a, 2019b).

To our knowledge, there is no direct measurement of reactive gaseous bromine and iodine species over China. Here we compare the measurement in the west Pacific (not within the domain of current study) and other similar environments with our simulation over the ocean outside of mainland China. Koenig et al. (2017) reported the observed levels of BrO and Br_y during a flight campaign in Jan to Feb, 2014. The mixing ratios of BrO at surface (<500 m) were between 0.15 to 1.7 pptv (daytime flight average) and those of Br_y were among 1.0 to 14.0 pptv. WRF-Chem model simulated a range of 0.01 to 1.5 pptv of BrO (daytime average) and 0.5 to 8 pptv of Bry (daytime average) in west Pacific in lower boundary layer. Saiz-Lopez and von Glasow (2012) compiled the available measurements of BrO around the world and reported the maximum values of 0.5 to 2.0 pptv for land-based sites and 3.0 to 3.6 pptv for cruises. WRF-Chem modeled seasonal average of daily-maximum BrO (Figure S3) typically between 0.5 to 2 pptv and Br_y (Figure 3) between 1 to 10 pptv, which is inline with the observations.

Großmann et al. (2013) carried out a cruise campaign in the western Pacific observing IO and they reported an average of 0.7 to 1.4 pptv (daytime flight average) of IO in the marine boundary layer in Oct, 2009. Prados-Roman, Cuevas, Fernandez, et al. (2015) reported an average of 0.4 to 1.4 pptv of IO from a global cruise campaign. WRF-Chem modeled a range of 0.75 to 2.5 pptv of IO (daytime average) in west Pacific. Saiz-Lopez and von Glasow (2012) summarized the previously reported IO observations to be 0.2 to 2.4 pptv from ground-based campaigns and about 3.5 pptv from ship measurements. WRF-Chem model predicted seasonal average of daily-maximum IO (Figure S3) to be 1.0 to 3.0 pptv and appears to be within the reasonable range.

Simulated levels of the reactive halogen species were in line with the measurements made in this region or similar environments. Therefore, the current model and setup is acceptable to investigate the effect of halogens on the individual oxidants and the overall oxidation capacity in China.

3.2. Impact of Halogens on Individual Oxidants

Figure 4 shows the annual average of the halogen impact on individual oxidants in China, and Figures 5, 6, 7, and 8 are the seasonal average for OH, HO_2, O_3, and NO_3, respectively. Halogen chemistry increases OH by up to 50% (annual average) in the polluted parts of China, especially in polluted coastal areas, e.g., Shanghai city in the Yangtze River Delta region (see Figure S1a for location). The increase of OH in polluted areas is primarily due to the enhanced production from the reactions of VOCs with chlorine atoms and the transformation of HO_2 into OH. Halogen-mediated differences in HO_2 have a similar pattern but with larger changes up to 84% (annual average). The reactions of halogen atoms with VOCs also result in an increase of HO_2 level in the polluted region. For the seasonal variation, the levels of OH and HO_2 peak in the summer for stronger radiation and photochemical reactions. The halogen-mediated relative influence on OH and HO_2, however, is largest during winter, because the chlorine emission is largest in winter season (section 3.1) and also the absolute level of OH and HO_2 in winter is lowest. The increase of HO_x due to halogens could be a missing source of OH, one of the critical questions in atmospheric photochemistry studies in China (e.g. Tan et al., 2017).

Zhang et al. (2017) updated the WRF-Chem model with chlorine chemistry and reported a net increase (up to 12%) of RO_x ($OH + HO_2 + RO_2$) at surface in China due to chlorine chemistry and anthropogenic chlorine emission. Wang et al. (2019) applied a global model (GEOS-Chem) without anthropogenic sources of chlorine and estimated the chlorine-driven effect on OH over China to be near-zero (over the land of east China) to slightly negative (over the coast). Sarwar et al. (2015) used a hemispheric version of CMAQ and predicted a slight decrease of OH (1%) and a significant decrease of HO_2 (11%) due to bromine and iodine chemistry in the northern hemisphere. Stone et al. (2018) used GEOS-Chem to evaluate the effect of bromine and iodine and found a slight increase (~2%) of OH and a decrease of HO_2 (−2% to −5%) over east China. Sherwen et al. (2016) used GEOS-Chem without inorganic chlorine (HCl and chloride aerosol) emissions from human activities and estimated the overall impact of halogens (Cl, Br, and I) on HO_x ($OH + HO_2$) over China to be near-zero to negative. In the marine atmosphere, the generally accepted overall impact of halogens on OH and HO_2 is transforming HO_2 to OH hence decreasing HO_2 and increasing OH, mostly driven by iodine and bromine chemistry (Saiz-Lopez & von Glasow, 2012). However, the present study shows that in polluted

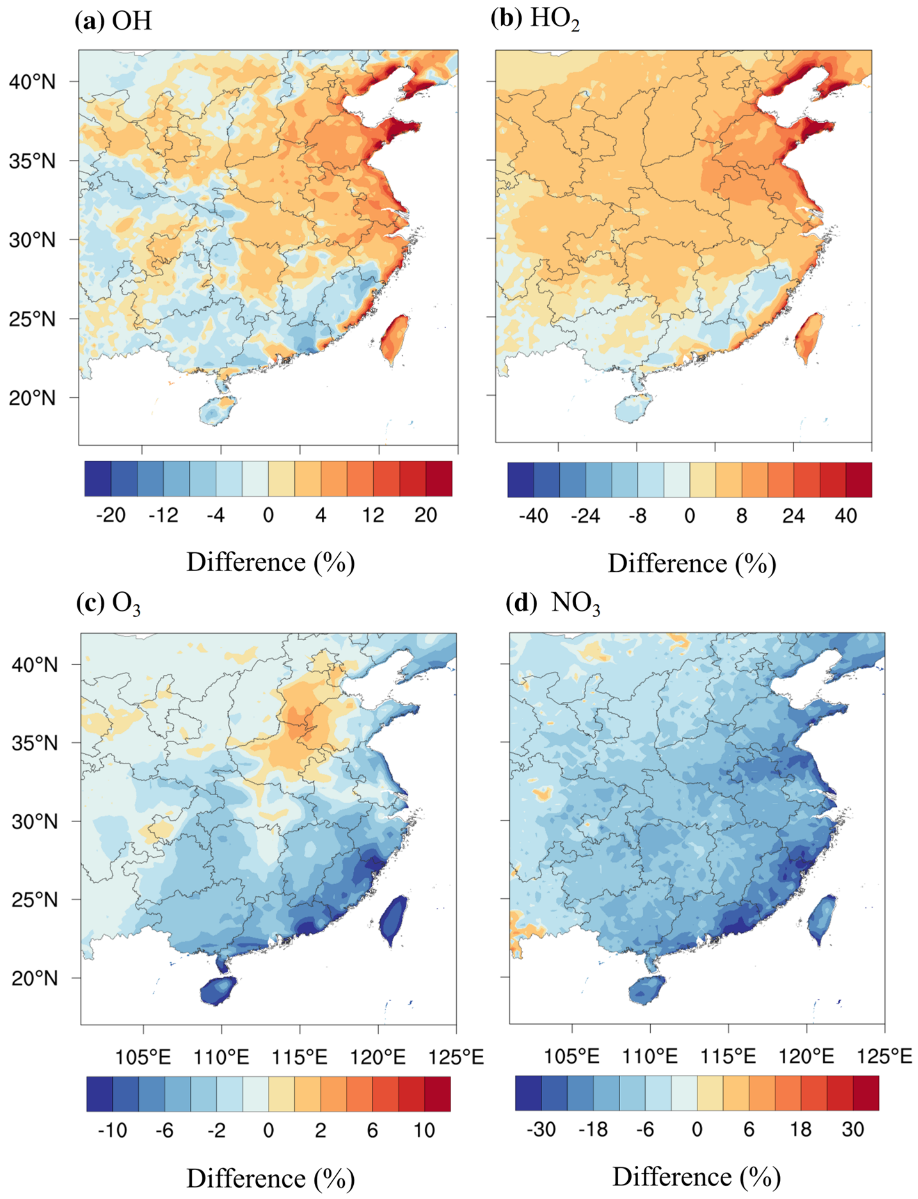

Figure 4. Annual average impact of halogen chemistry on the level of atmospheric oxidants at the surface in China. Note the different scales in the four species. **A** halogen chemistry significantly increases the OH level in polluted China but decreases OH in the rural area. **B** the difference of HO_2 induced by halogens is similar to that of OH but with higher changes. **C** the addition of halogen chemistry results in a considerable reduction of O_3 in most regions and an enhancement effect in northern China. **D** NO_3 is significantly reduced across the country due to halogen chemistry.

parts of China, OH and HO_2 changes due to halogens remain mostly positive suggesting that the increase effect of chlorine on HO_x surpasses the transforming effect caused by bromine and iodine (Figure S4).

Surface O_3 is slightly increased by ~2% (annual average) by halogens in northern China and is decreased in other regions (by as much as −16%) (Figure 4). For the seasonal variation (Figure 7), O_3 is reduced by halogens in summer across the country by as much as −23%. In contrast, O_3 is enhanced in the winter season by up to 18% in a significant portion of China. Noticeably, including halogen chemistry reduces the difference of maximum daily 8-h average (MDA8) O_3 between simulation and observation by up to 8 ppb (mostly ranging from 0.1 to 3 ppb) at the locations of ~550 observational sites in China (Figure S2).

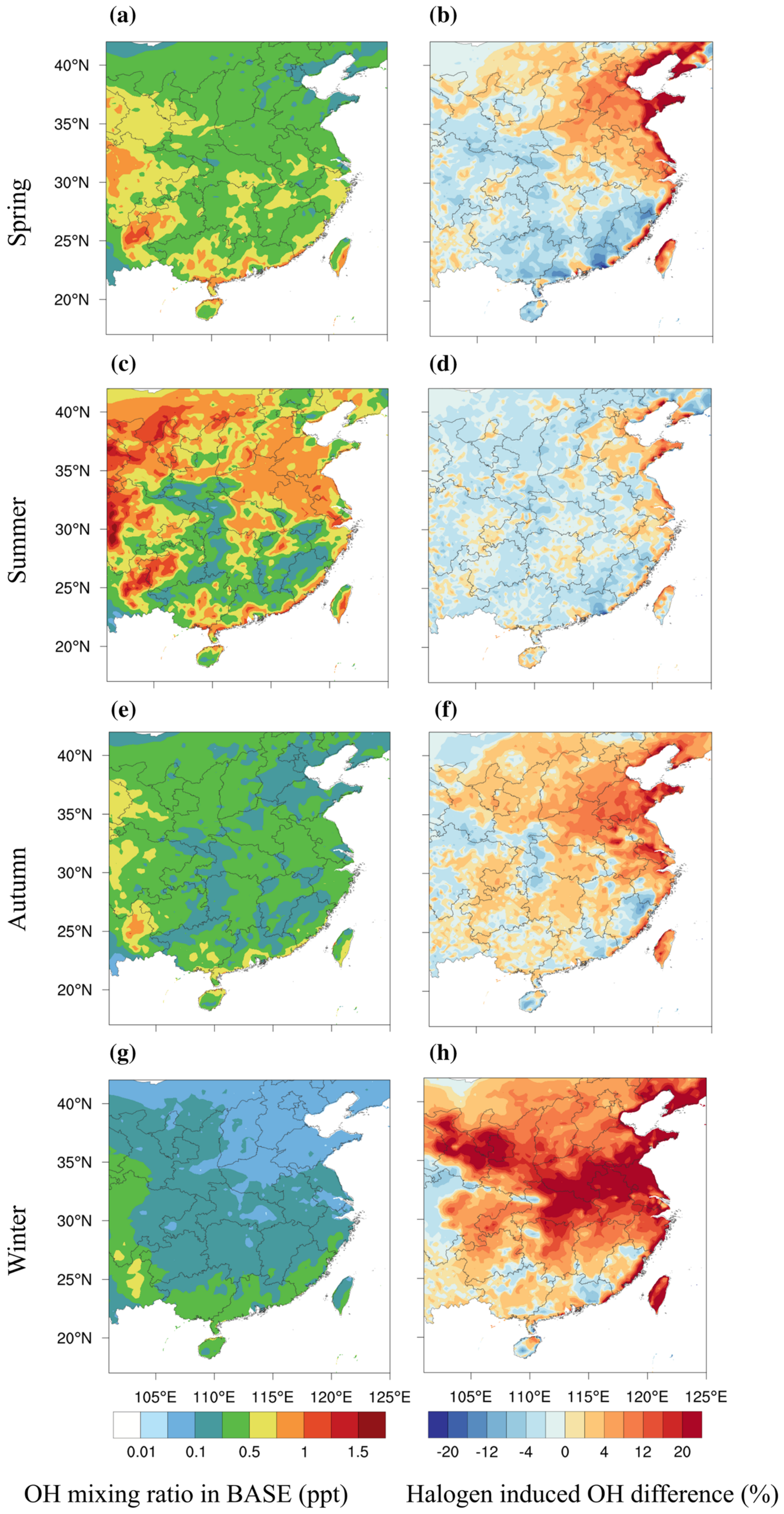

Figure 5. Seasonal average of daily-maximum OH at the surface in the BASE scenario and relative changes due to halogens (difference between HAL-BASE) in the four seasons.

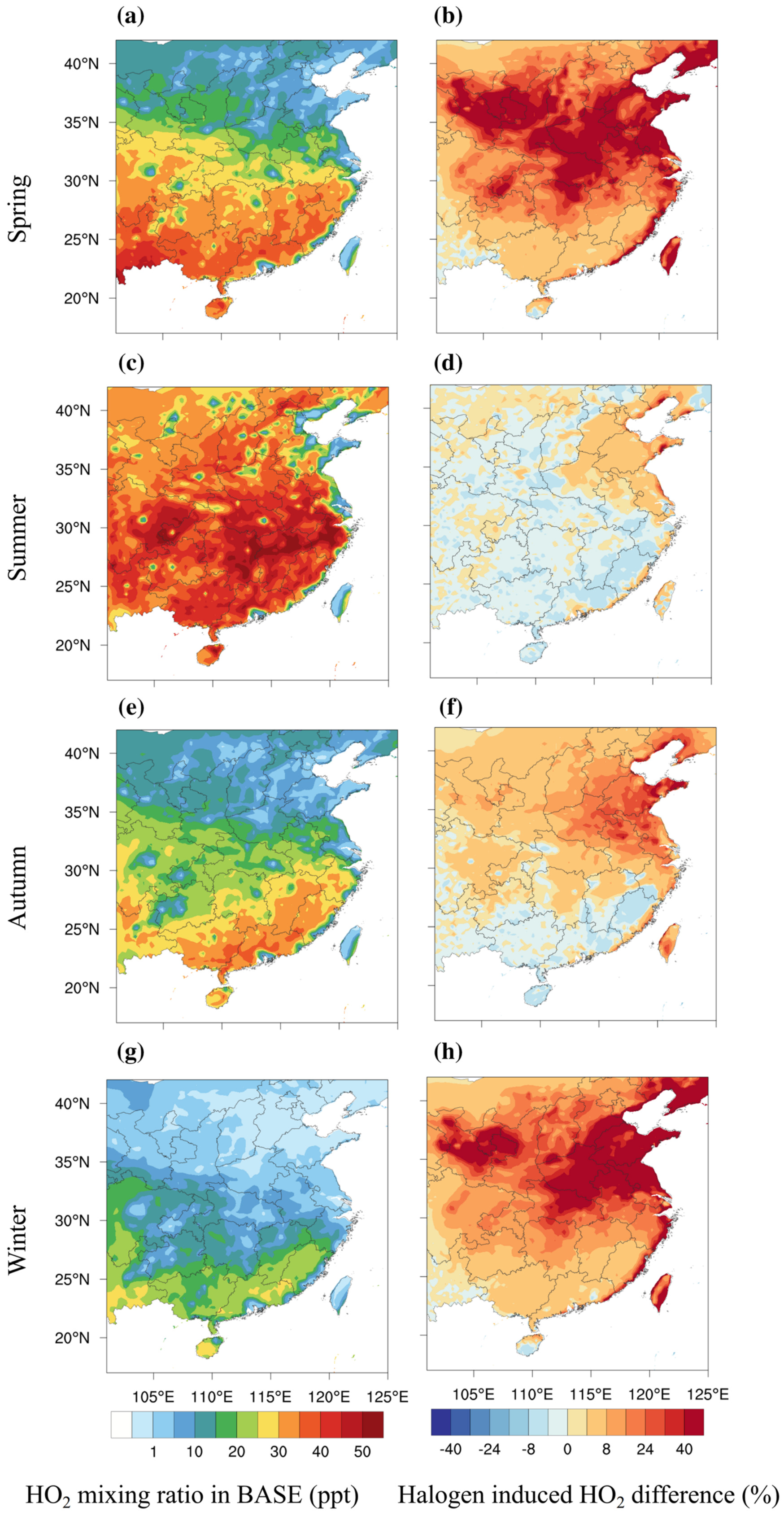

Figure 6. The same as Figure 5, but for HO_2.

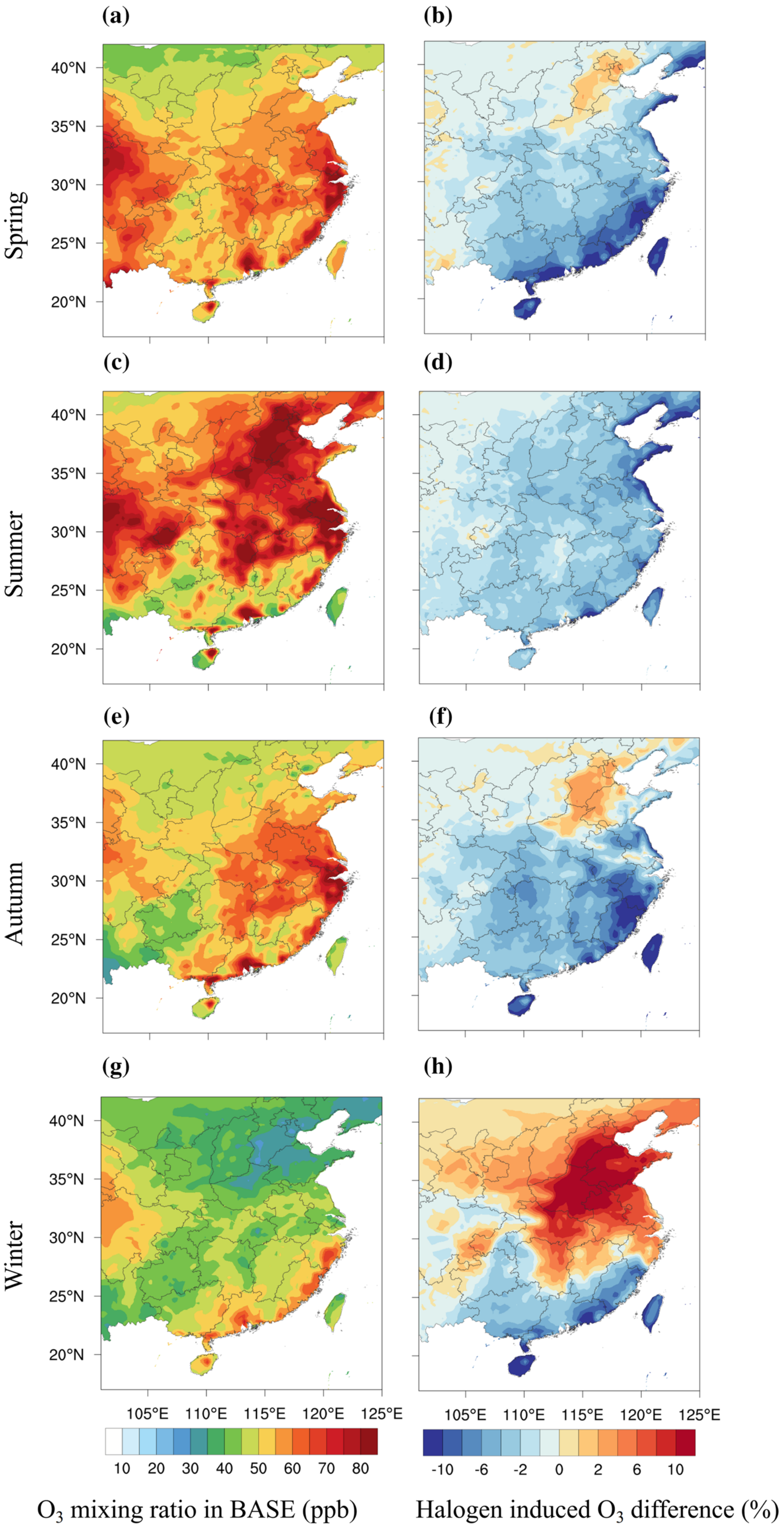

Figure 7. The same as Figure 5, but for O_3.

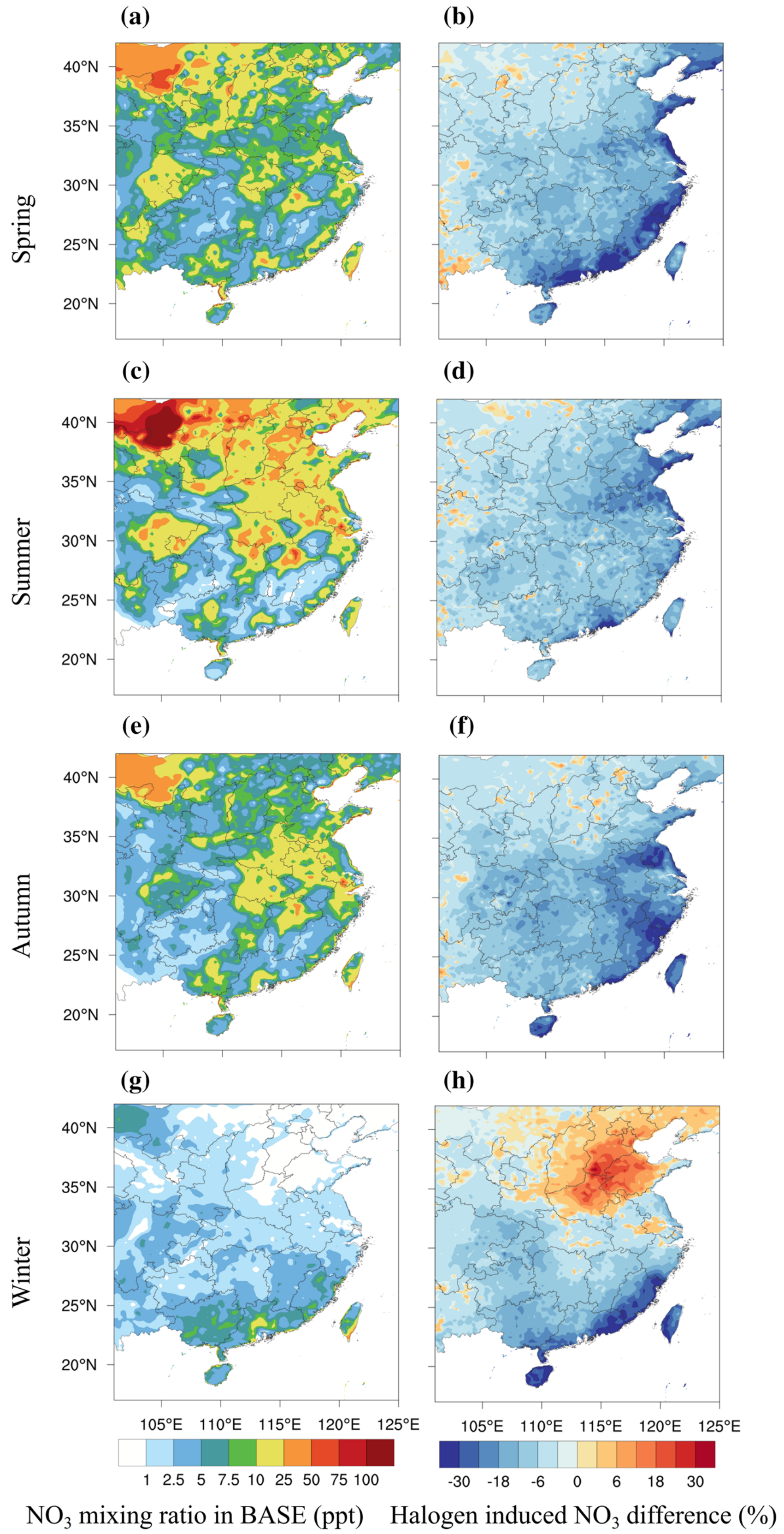

Figure 8. The same as Figure 5, but for NO$_3$.

The enhancement effect of chlorine on O_3 in polluted regions and the decreasing effect of bromine and iodine have been well established, and hence the overall influence of halogens on surface O_3 is currently thought to be negative. For the chlorine effect, Sarwar et al. (2014) applied the hemispheric version of the CMAQ model and predicted an increase of up to 7.0 ppbv of MDA8 O_3 in Europe and China. Li et al. (2016) implemented the $ClNO_2$ production in WRF-Chem and reported a significant increase of O_3 levels (up to 7.23 ppbv or 16.3%) in China. Wang et al. (2019) updated the chlorine chemistry in GEOS-Chem and found neutral to negative effect of chlorine chemistry and natural chlorine sources on O_3 in China. Note that Wang et al. (2019) did not include the anthropogenic chlorine in their assessment because the use of a global chlorine emission inventory (RCEI, Keene et al., 1999) overestimated the observed chlorine species on a global scale in their model. For the bromine and iodine effect, Sarwar et al. (2015) reported a reduction of surface O_3 by 2 to 4 ppbv over terrestrial areas and about 6 ppbv over ocean regions in the northern hemisphere. As to the combined effect of halogens, Sherwen et al. (2016) estimated a large decrease of surface O_3 especially over ocean (30.0%) and around 5–10% over China. Sherwen et al. (2017) employed the GEOS-Chem model in a regional configuration for Europe and found a large reduction of surface O_3 (up to 28.9 ppbv; in average 13.5 ppbv) in summer 2015 over Europe due to halogens. Li, Borge, et al. (2019) applied a revised CMAQ with comprehensive halogen chemistry and sources in Europe and estimated a decrease of over 3.0 ppbv in summer 2016 in coastal Europe. However, in the present study in northern China, we find that the destructive effect of bromine and iodine on O_3 can be compensated for, or even overwhelmed by, the enhancement effect of chlorine (Figure S4) .

The effect of halogens on the main nighttime oxidant, NO_3, is somewhat similar to that on O_3. NO_3 is significantly reduced by halogens as much as 42% (annual average) across China (Figure 4). As to the seasonal variation (Figure 8), NO_3 is reduced significantly across China except in winter season in northern China. NO_3 radical is formed from the reaction of NO_2 and O_3, and is primarily removed by photolysis reaction during daytime, reactions with some VOC species, reactions with radicals including halogen atoms, and reaction with NO_2 to form N_2O_5 and ultimately HNO_3 and nitrate aerosol. The changes of nitrate radical in the current work are caused by the combination of the following effects: (1) halogens significantly reduces O_3 except in winter in the northern part of China; (2) halogens induced complex changes NO_2 (Figure S5) because halogen oxides transform NO to NO_2, remove NO_2 to halogen nitrates, and extend the lifetime of NO_2 by forming XNO_2 (from halogen reactions with N_2O_5 which would otherwise be lost to HNO_3); (3) halogens (Br, I, and I_2) directly reacts with NO_3 and reduce the level of this nighttime radical. Muñiz-Unamunzaga et al. (2018) adopted the CMAQ model and reported a large decrease of NO_3 (20–50%) due to halogen chemistry in September 2006 in Los Angeles, United States.

3.3. Impact of Halogens on Oxidation Capacity

3.3.1. Overall Impact

The estimated AOC in the BASE scenario (i.e., without halogens) is mostly in the range of 10^7 to 10^8 # $cm^{-3} s^{-1}$ in China (Figure S6) with an annual average of $2.2x10^7$ # cm^{-3} s^{-1}. AOC has a diurnal pattern (Figure S7): (1) AOC in daytime is approximately 5 to 10 times higher than that at night; (2) AOC in daytime (dominated by OH) peaks during morning traffic rush hours or at noon which suggests the critical role of reactant or oxidant levels; (3) AOC in nighttime (controlled by O_3 and NO_3) gradually drops before reaching a minimum at dawn.

The halogen-mediated effect on AOC, hereafter referred to as HAOC, shows considerable spatio-temporal heterogeneity (Figure 9). Note that this is the first attempt to evaluate HAOC. HAOC is consistently positive throughout the year in the polluted regions in China (see Figure S1b for the locations of polluted areas) typically between 10% and 20% (up to 87% in the winter season). HAOC also presents a clear diurnal pattern (Figure S7). HAOC in daytime is predominantly positive via increasing OH and adding Cl radical. HAOC at night is mostly negative through decreasing the levels of O_3 and NO_3. As to the 24 h averaged HAOC (Figure 9), it is positive in polluted regions and negative in cleaner areas.

3.3.2. Oceanic and Anthropogenic Impact

Oceanic sources of RHS result in noticeable levels of bromine (Br_y) and iodine (I_y) over the ocean and a non-negligible fraction (>0.5 pptv) over the land. Oceanic sources mainly cause increases of HAOC (Figure 10) via increasing the level of OH (R7 and R8) in the coastal area with strongest influence during

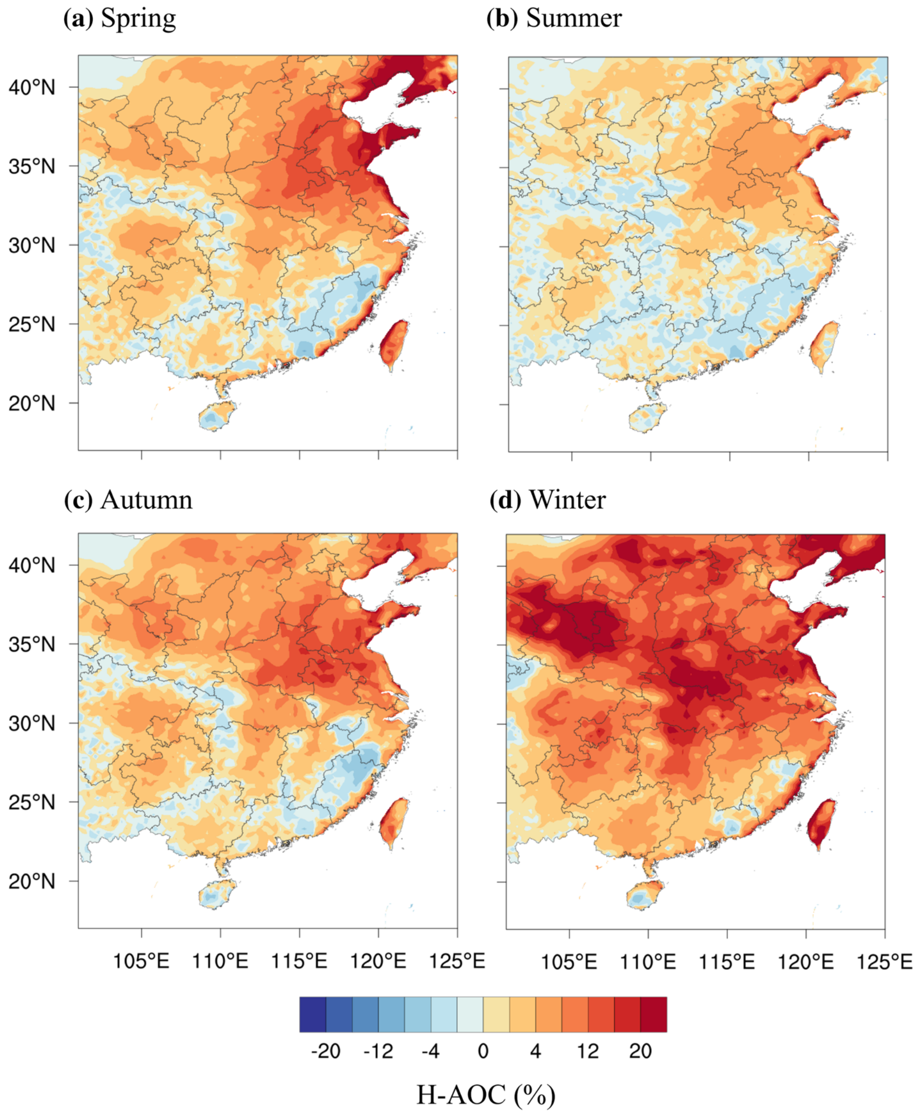

Figure 9. Impact of halogen chemistry on the atmospheric oxidation capacity at the surface in China. **A** HAOC in spring is positive in cities but negative in rural areas. **B** HAOC in summer is similar to that in spring but with less intensive impact. **C** HAOC in autumn is similar to that in spring. **D** winter HAOC is positive throughout the country.

Spring season (up to 75%). The significant influence of oceanic sources of halogens should be included in the air quality studies in Chinese coastal regions.

Anthropogenic (land) chlorine emissions (e.g., from burning coal, biomass, and municipal solid waste) result in hot spots of reactive chlorine species (Cl_y) mainly in the polluted parts of China. Anthropogenic emission of chlorine further induces (on top of the oceanic influence) significant and widespread enhancement of HAOC over mainland China with the largest increase in winter (up to 49%). Immediate actions should be taken in controlling the anthropogenic chlorine emission. Xue et al. (2015) updated the chlorine reactions in a box model (MCM) and applied it in China to evaluate the effect of the chlorine chemistry (mostly $ClNO_2$) on atmospheric oxidative capacity and they found an increase of 25.4% (daytime average) using measurement data at one site in Hong Kong, China, in summer season.

We also calculate the contributions of iodine species to the total HAOC to be up to 29%. Additional relevance comes from the fact that the global dominant source of iodine has increased in recent decades due to the

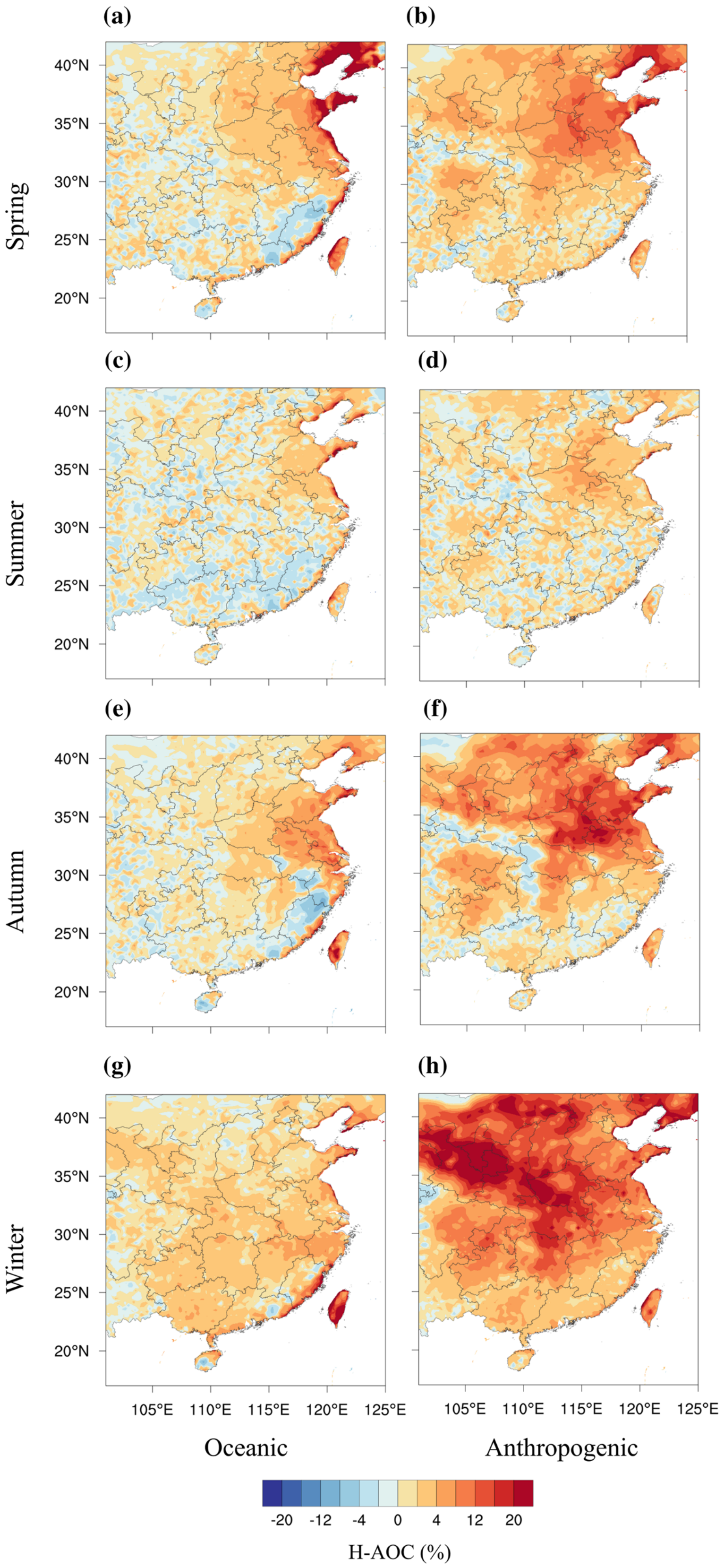

Figure 10. Impact of oceanic and anthropogenic sources of halogens on atmospheric oxidation capacity at the surface in China.

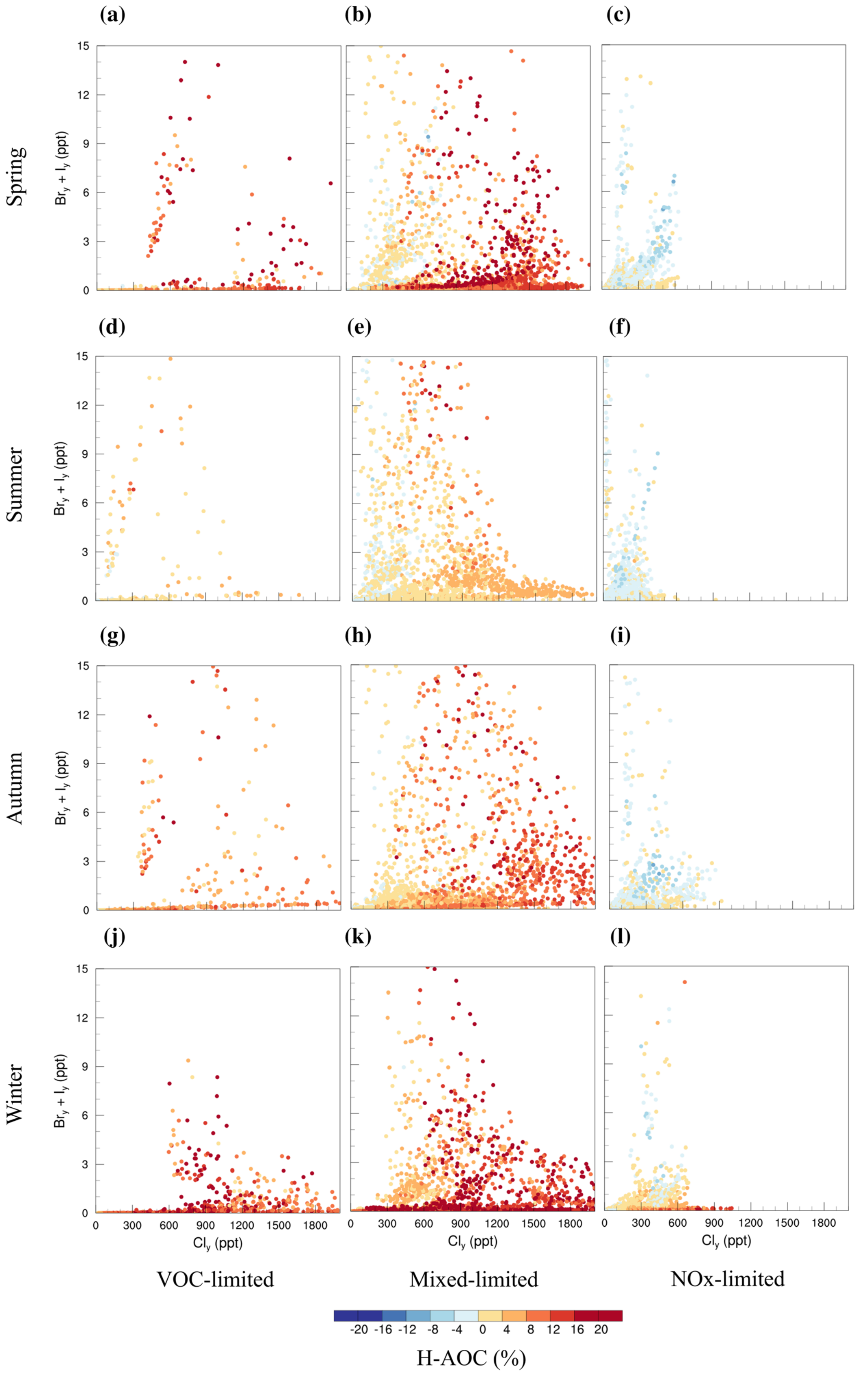

Figure 11. Dependence of HAOC on the levels of halogen species under different O_3 formation regimes in four seasons.

deposition to the ocean of increasing anthropogenic O_3 and the subsequent oxidation of seawater iodide to HOI and I_2 released to the atmosphere (Cuevas et al., 2018; Legrand et al., 2018). Such feedback between atmospheric O_3 pollution and iodine emissions is thought to have partially buffered the increases in tropospheric O_3 relative to pre-industrial levels (Prados-Roman, Cuevas, Hay, et al., 2015). Driven by increasing anthropogenic ozone (Young et al., 2013), ocean iodine emissions are expected to increase in the future (Cuevas et al., 2018), and their impact on atmospheric oxidation in China is thus expected to increase as a result of anthropogenic pollution feedbacks.

3.4. Connection Between O_3 Formation Regime and HAOC

A profound characteristic of O_3 formation and radical cycling is the different responses of O_3 production to the changes of its precursors (NO_x and VOC) in different O_3 regimes. In the region with excessive NO_x or insufficient VOC (VOC-limited), the HO_x (OH, HO_2) radical budget is mostly controlled by NO_x (via the reaction of OH with NO_2), so decreasing NO_x level increases the level of HO_x radicals, hence the formation of O_3 and NO_3. Meanwhile, in the region with excessive VOC or insufficient NO_x (NO_x-limited), the HO_x radical budget is controlled by bi-radical reactions, and an increase of NO_x leads to enhanced production of O_3 and thus OH and NO_3 (Li et al., 2018; Sillman & West, 2009). The impact of halogens on AOC (via influencing the individual oxidant) is therefore closely related to the O_3 formation regime.

We used the seasonal average simulation results to separate the regions within our domain into three categories (Dodge, 1977): VOC-limited (VOC/NO_x lower than 4, the region with red dots in Figure S1e and S1f), NO_x-limited (VOC/NO_x over 15, the region with blue dots), and mixed-limited (VOC/NO_x between 4 and 15, the region with yellow dots). VOC-limited regions are basically the urban and industrial areas (regions with elevated NO_2 concentration) whereas NO_x-limited and mixed-limited regions are rural and suburban areas, respectively.

We find that HAOC is closely related to the O_3 formation chemical regime (Figure 11). HAOC in VOC-limited regions shows an increase pattern in all seasons; and in mixed-limited regions, HAOC is significantly increased when Cl_y is over 600 pptv (typical value over polluted China, Figure 3) or when $Br_y + I_y$ levels are negligible, and is near zero or decreased when Cl_y is lower than 600 pptv; and in NO_x-limited regions, HAOC is generally decreased except in winter, when the levels of bromine and iodine species are negligible in mainland China. A dynamic strategy is required to curb the enhancement effect of halogens on AOC under various O_3 regimes.

4. Conclusions and Final Remarks

The results reveal the significant control of halogens on atmospheric oxidation, the levels of oxidants and air pollutants in China, which potentially contributes to close the current gap between the observation and simulation of atmospheric oxidation in China. This large oxidation enhancement effect is currently omitted from air pollution modeling in China, which implies a fundamental gap in our understanding of air pollution in this region and a potential bias in policy design. One of the implications is the effect of halogens on the O_3 response to the changing emissions of VOC and NO_x, considering that halogens significantly perturb the level of oxidants, the oxidation of VOC, and the budget of NO_x which were reported to change O_3 sensitivity (Li et al., 2018).

Pollutants in China can be horizontally transported to the Pacific Ocean and North America (Verstraeten et al., 2015) and vertically transported to the upper troposphere and lower stratosphere (Randel et al., 2010). Therefore, halogens also affect China's air pollution exports to other parts of the world.

Although the present study merely shows the impact of halogens in China, a similar large influence is also expected in other regions with similar air quality issues and halogen emissions from anthropogenic and oceanic sources, e.g., India, Southeast Asia, Mexico, and South America, among others. The emission of halogens (and hence its impact on atmospheric oxidation) is expected to increase as a result of the projected natural phenomena (Iglesias-Suarez et al., 2020) and anthropogenic activity (Fang et al., 2019; Young et al., 2013) which warrants further investigation of the influence of halogen compounds on future atmospheric oxidation.

Disclaimer

The views expressed in this paper are those of the authors and do not necessarily represent the views or policies of the U.S. EPA.

Acknowledgments
This study received funding from the European Research Council Executive Agency under the European Union's Horizon 2020 Research and Innovation Programme (Project ERC-2016- COG 726349 CLIMAHAL), and was supported by the Consejo Superior de Investigaciones Científicas (CSIC) of Spain, and The Program for Professor of Special Appointment (Eastern Scholar) at Shanghai Institutions of Higher Learning and Shanghai Thousand Talents Program. The development and maintenance of the WRF-Chem model are conducted by NOAA/ESRL/GSD in active collaboration with other institutes. Computing resources, support, and data storage were provided by the Climate Simulation Laboratory at NCAR's Computational and Information Systems Laboratory (CISL), sponsored by the NSF. The Fudan team acknowledges the financial support from National Natural Science Foundation of China (41775113). The HKPU team acknowledges financial support from the Hong Kong Research Grants Council (A-PolyU502/16, T24-504/17-N). Data that support the finding of this study can be found at DOI: 10.17632/whz6yk79m4.1 (Li et al., 2020).

References

Badia, A., Reeves, C. E., Baker, A. R., Saiz-Lopez, A., Volkamer, R., Koenig, T. K., et al. (2019). Importance of reactive halogens in the tropical marine atmosphere: A regional modelling study using WRF-Chem. *Atmospheric Chemistry and Physics*, *19*(5), 3161–3189. https://doi.org/10.5194/acp-19-3161-2019

Carpenter, L. J., MacDonald, S. M., Shaw, M. D., Kumar, R., Saunders, R. W., Parthipan, R., et al. (2013). Atmospheric iodine levels influenced by sea surface emissions of inorganic iodine. *Nature Geoscience*, *6*(2), 108–111. https://doi.org/10.1038/ngeo1687

Chen, F., & Dudhia, J. (2001). Coupling an advanced land surface–hydrology model with the Penn State–NCAR MM5 modeling system. Part I: Model implementation and sensitivity. *Monthly Weather Review*, *129*(4), 569–585.

Cuevas, C. A., Maffezzoli, N., Corella, J. P., Spolaor, A., Vallelonga, P., Kjær, H. A., et al. (2018). Rapid increase in atmospheric iodine levels in the North Atlantic since the mid-20th century. *Nature Communications*, *9*(1), 1452. https://doi.org/10.1038/s41467-018-03756-1

Dodge, M.C. (1977). Combined use of modeling techniques and smog chamber data to derive ozone—Precursor relationships. International Conference on Photochemical Oxidant Pollution and its Control: Proceedings, Vol. II., B. EPA/600/3–77-001b. U. S. Environmental Protection Agency, Environmental Sciences Research Laboratory, Research Triangle Park, N.C., 881—889.

Emmons, L. K., Walters, S., Hess, P. G., Lamarque, J. F., Pfister, G. G., Fillmore, D., et al. (2010). Description and evaluation of the model for ozone and related chemical tracers, version 4 (MOZART-4). *Geoscientific Model Development*, *3*(1), 43–67. https://doi.org/10.5194/gmd-3-43-2010

Fang, X., Park, S., Saito, T., Tunnicliffe, R., Ganesan, A. L., Rigby, M., et al. (2019). Rapid increase in Li, Qinyi; Badia, Alba; Wang, Tao; Sarwar, Golam; Fu, Xiao; Zhang, Li; Zhang, Qiang; Fung, Jimmy; Cuevas, Carlos; Wang, Shanshan; Zhou, bin; Saiz-Lopez, Alfonso (2020), "potential effect of halogens on atmospheric oxidation and air quality in China", Mendeley data, v1ozone-depleting chloroform emissions from China. *Nature Geoscience*, *12*, 89–93.

Fernandez, R. P., Salawitch, R. J., Kinnison, D. E., Lamarque, J. F., & Saiz-Lopez, A. (2014). Bromine partitioning in the tropical tropopause layer: Implications for stratospheric injection. *Atmospheric Chemistry and Physics*, *14*(24), 13,391–13,410.

Fu, X., Wang, T., Wang, S., Zhang, L., Cai, S., Xing, J., & Hao, J. (2018). Anthropogenic emissions of hydrogen chloride and fine particulate chloride in China. *Environmental Science & Technology*, *52*(3), 1644–1654. https://doi.org/10.1021/acs.est.7b05030

Fu, Y., Liao, H., & Yang, Y. (2019). Interannual and decadal changes in tropospheric ozone in China and the associated chemistry-climate interactions: A review. *Advances in Atmospheric Sciences*, *36*(9), 975–993.

Glasow, R. V., Kuhlmann, R. V., Lawrence, M. G., Platt, U., & Crutzen, P. J. (2004). Impact of reactive bromine chemistry in the troposphere. *Atmospheric Chemistry and Physics*, *4*(11/12), 2481–2497.

Grell, G. A., Peckham, S. E., Schmitz, R., McKeen, S. A., Frost, G., Skamarock, W. C., & Eder, B. (2005). Fully coupled "online" chemistry within the WRF model. *Atmospheric Environment*, *39*(37), 6957–6975.

Großmann, K., Frieß, U., Peters, E., Wittrock, F., Lampel, J., Yilmaz, S., et al. (2013). Iodine monoxide in the Western Pacific marine boundary layer. *Atmospheric Chemistry and Physics*, *13*(6), 3363–3378. https://doi.org/10.5194/acp-13-3363-2013

Hossaini, R., Chipperfield, M. P., Saiz-Lopez, A., Fernandez, R., Monks, S., Feng, W., et al. (2016). A global model of tropospheric chlorine chemistry: Organic versus inorganic sources and impact on methane oxidation. *Journal of Geophysical Research: Atmospheres*, *121*, 14–271. https://doi.org/10.1002/2016JD025756

Iacono, M. J., Delamere, J. S., Mlawer, E. J., Shephard, M. W., Clough, S. A., & Collins, W. D. (2008). Radiative forcing by long-lived greenhouse gases: Calculations with the AER radiative transfer models. *Journal of Geophysical Research*, *113*, D13103. https://doi.org/10.1029/2008JD009944

Iglesias-Suarez, F., Badia, A., Fernandez, R. P., Cuevas, C. A., Kinnison, D. E., Tilmes, S., et al. (2020). Natural halogens buffer tropospheric ozone in a changing climate. *Nature Climate Change*, *10*(2), 147–154. https://doi.org/10.1038/s41558-019-0675-6

Janjić, Z. I. (1994). The step-mountain eta coordinate model: Further developments of the convection, viscous sublayer, and turbulence closure schemes. *Monthly Weather Review*, *122*(5), 927–945.

Karamchandani, P., Zhang, Y., Chen, S. Y., & Balmori–Bronson, R. (2012). Development of an extended chemical mechanism for global–through–urban applications. *Atmospheric Pollution Research*, *3*(1), 1–24.

Keene, W. C., Khalil, M. A. K., Erickson, D. J., III, McCulloch, A., Graedel, T. E., Lobert, J. M., et al. (1999). Composite global emissions of reactive chlorine from anthropogenic and natural sources: Reactive Chlorine Emissions Inventory. *Journal of Geophysical Research: Atmospheres*, *104*(D7), 8429–8440.

Koenig, T. K., Volkamer, R., Baidar, S., Dix, B., Wang, S., Anderson, D. C., et al. (2017). BrO and inferred Bry profiles over the western Pacific: Relevance of inorganic bromine sources and a Bry minimum in the aged tropical tropopause layer. *Atmospheric Chemistry and Physics*, *17*(24), 15,245–15,270. https://doi.org/10.5194/acp-17-15245-2017

Legrand, M., McConnell, J. R., Preunkert, S., Arienzo, M., Chellman, N., Gleason, K., et al. (2018). Alpine ice evidence of a three-fold increase in atmospheric iodine deposition since 1950 in Europe due to increasing oceanic emissions. *Proceedings of the National Academy of Sciences*, *115*(48), 12,136–12,141. https://doi.org/10.1073/pnas.1809867115

Lelieveld, J., Evans, J. S., Fnais, M., Giannadaki, D., & Pozzer, A. (2015). The contribution of outdoor air pollution sources to premature mortality on a global scale. *Nature*, *525*(7569), 367–371. https://doi.org/10.1038/nature15371

Li, Q., Badia, A., Wang, T., Sarwar, G., Fu, X., Zhang, L., et al. (2020). Potential Effect of Halogens on Atmospheric Oxidation and Air Quality in China, Mendeley Data, v1. https://doi.org/10.17632/whz6yk79m4.1

Li, K., Jacob, D. J., Liao, H., Shen, L., Zhang, Q., & Bates, K. H. (2019). Anthropogenic drivers of 2013–2017 trends in summer surface ozone in China. *Proceedings of the National Academy of Sciences*, *116*(2), 422–427.

Li, Q., Borge, R., Sarwar, G., de la Paz, D., Gantt, B., Domingo, J., et al. (2019). Impact of halogen chemistry on summertime air quality in coastal and continental Europe: Application of the CMAQ model and implications for regulation. *Atmospheric Chemistry and Physics*, *19*(24), 15,321–15,337. https://doi.org/10.5194/acp-19-15321-2019

Li, Q., Zhang, L., Tham, Y. J., Ahmadov, R., Xue, L., Zhang, Q., & Zheng, J. (2016). Impacts of heterogeneous uptake of dinitrogen pentoxide and chlorine activation on ozone and reactive nitrogen partitioning: Improvement and application of the WRF-Chem model in southern China. *Atmospheric Chemistry and Physics*, *16*(23), 14,875.

Li, Q., Zhang, L., Wang, T., Wang, Z., Fu, X., & Zhang, Q. (2018). "New" reactive nitrogen chemistry reshapes the relationship of ozone to its precursors. *Environmental Science & Technology*, *52*(5), 2810–2818. https://doi.org/10.1021/acs.est.7b05771

Liss, P. S., & Slater, P. G. (1974). Flux of gases across the Air-Sea Interface. *Nature*, *247*(5438), 181–184.

Lu, K., Guo, S., Tan, Z., Wang, H., Shang, D., Liu, Y., et al. (2018). Exploring atmospheric free-radical chemistry in China: The self-cleansing capacity and the formation of secondary air pollution. *National Science Review*, *6*(3), 579–594.

McDuffie, E. E., Fibiger, D. L., Dubé, W. P., Lopez-Hilfiker, F., Lee, B. H., Thornton, J. A., et al. (2018). Heterogeneous N2O5 uptake during WINTER: Aircraft measurements during the 2015 WINTER campaign and critical evaluation of current parameterizations. *Journal of Geophysical Research: Atmospheres*, *123*, 4345–4372. https://doi.org/10.1002/2018JD028336

Monks, P. S., Archibald, A. T., Colette, A., Cooper, O., Coyle, M., Derwent, R., et al. (2015). Tropospheric ozone and its precursors from the urban to the global scale from air quality to short-lived climate forcer. *Atmospheric Chemistry and Physics*, *15*(15), 8889–8973. https://doi.org/10.5194/acp-15-8889-2015

Morrison, H., Thompson, G., & Tatarskii, V. (2009). Impact of cloud microphysics on the development of trailing stratiform precipitation in a simulated squall line: Comparison of one-and two-moment schemes. *Monthly Weather Review*, *137*(3), 991–1007.

Muñiz-Unamunzaga, M., Borge, R., Sarwar, G., Gantt, B., de la Paz, D., Cuevas, C. A., & Saiz-Lopez, A. (2018). The influence of ocean halogen and sulfur emissions in the air quality of a coastal megacity: The case of Los Angeles. *Science of the Total Environment*, *610*, 1536–1545.

Ordóñez, C., Lamarque, J. F., Tilmes, S., Kinnison, D. E., Atlas, E. L., Blake, D. R., et al. (2012). Bromine and iodine chemistry in a global chemistry-climate model: Description and evaluation of very short-lived oceanic sources. *Atmospheric Chemistry and Physics*, *12*(3), 1423–1447. https://doi.org/10.5194/acp-12-1423-2012

Prados-Roman, C., Cuevas, C. A., Fernandez, R. P., Kinnison, D. E., Lamarque, J. F., & Saiz-Lopez, A. (2015). A negative feedback between anthropogenic ozone pollution and enhanced ocean emissions of iodine. *Atmospheric Chemistry and Physics*, *15*(4), 2215–2224.

Prados-Roman, C., Cuevas, C. A., Hay, T., Fernandez, R. P., Mahajan, A. S., Royer, S. J., et al. (2015). Iodine oxide in the global marine boundary layer. *Atmospheric Chemistry and Physics*, *15*(2), 583–593. https://doi.org/10.5194/acp-15-583-2015

Qiu, X., Ying, Q., Wang, S., Duan, L., Wang, Y., Lu, K., et al. (2019b). Significant impact of heterogeneous reactions of reactive chlorine species on summertime atmospheric ozone and free-radical formation in North China. *Science of the Total Environment*, *693*, 133580. https://doi.org/10.1016/j.scitotenv.2019.133580

Qiu, X., Ying, Q., Wang, S., Duan, L., Zhao, J., Xing, J., et al. (2019a). Modeling the impact of heterogeneous reactions of chlorine on summertime nitrate formation in Beijing, China. *Atmospheric Chemistry and Physics*, *19*(10), 6737–6747. https://doi.org/10.5194/acp-19-6737-2019

Randel, W. J., Park, M., Emmons, L., Kinnison, D., Bernath, P., Walker, K. A., et al. (2010). Asian monsoon transport of pollution to the stratosphere. *Science*, *328*(5978), 611–613. https://doi.org/10.1126/science.1182274

Saiz-Lopez, A., Fernandez, R. P., Ordóñez, C., Kinnison, D. E., Gómez Martín, J. C., Lamarque, J. F., & Tilmes, S. (2014). Iodine chemistry in the troposphere and its effect on ozone. *Atmospheric Chemistry and Physics*, *14*(23), 13,119–13,143.

Saiz-Lopez, A., & von Glasow, R. (2012). Reactive halogen chemistry in the troposphere. *Chemical Society Reviews*, *41*(19), 6448–6472. https://doi.org/10.1039/c2cs35208g

Sarwar, G., Gantt, B., Schwede, D., Foley, K., Mathur, R., & Saiz-Lopez, A. (2015). Impact of enhanced ozone deposition and halogen chemistry on tropospheric ozone over the northern hemisphere. *Environmental Science & Technology*, *49*(15), 9203–9211. https://doi.org/10.1021/acs.est.5b01657

Sarwar, G., Simon, H., Xing, J., & Mathur, R. (2014). Importance of tropospheric ClNO2 chemistry across the northern hemisphere. *Geophysical Research Letters*, *41*, 4050–4058. https://doi.org/10.1002/2014GL059962

Seinfeld, J. H. & Pandis, S. N. (2006). Atmospheric Chemistry and Physics: From Air Pollution to Climate Change, Second Edition.

Sherwen, T., Evans, M. J., Sommariva, R., Hollis, L. D. J., Ball, S. M., Monks, P. S., et al. (2017). Effects of halogens on European air-quality. *Faraday Discussions*, *200*, 75–100. https://doi.org/10.1039/c7fd00026j

Sherwen, T., Schmidt, J. A., Evans, M. J., Carpenter, L. J., Großmann, K., Eastham, S. D., et al. (2016). Global impacts of tropospheric halogens (cl, Br, I) on oxidants and composition in GEOS-Chem. *Atmospheric Chemistry and Physics*, *16*(18), 12,239–12,271. https://doi.org/10.5194/acp-16-12239-2016

Sillman, S., & West, J. J. (2009). Reactive nitrogen in Mexico City and its relation to ozone-precursor sensitivity: Results from photochemical models. *Atmospheric Chemistry and Physics*, *9*(11), 3477–3489.

Simpson, W. R., Brown, S. S., Saiz-Lopez, A., Thornton, J. A., & von Glasow, R. (2015). Tropospheric halogen chemistry: Sources, cycling, and impacts. *Chemical Reviews*, *115*(10), 4035–4062.

Solomon, S. (1999). Stratospheric ozone depletion: A review of concepts and history. *Reviews of Geophysics*, *37*(3), 275–316.

Stone, D., Sherwen, T., Evans, M. J., Vaughan, S., Ingham, T., Whalley, L. K., et al. (2018). Impacts of bromine and iodine chemistry on tropospheric OH and HO2: Comparing observations with box and global model perspectives. *Atmospheric Chemistry and Physics*, *18*(5), 3541–3561. https://doi.org/10.5194/acp-18-3541-2018

Tan, Z., Fuchs, H., Lu, K., Hofzumahaus, A., Bohn, B., Broch, S., et al. (2017). Radical chemistry at a rural site (Wangdu) in the North China plain: Observation and model calculations of OH, HO 2 and RO 2 radicals. *Atmospheric Chemistry and Physics*, *17*(1), 663–690.

Tan, Z., Lu, K., Jiang, M., Su, R., Wang, H., Lou, S., et al. (2019). Daytime atmospheric oxidation capacity in four Chinese megacities during the photochemically polluted season: A case study based on box model simulation. *Atmospheric Chemistry and Physics*, *19*(6), 3493–3513. https://doi.org/10.5194/acp-19-3493-2019

Tham, Y. J., Wang, Z., Li, Q., Wang, W., Wang, X., Lu, K., et al. (2018). Heterogeneous N2O5 uptake coefficient and production yield of ClNO2 in polluted northern China: Roles of aerosol water content and chemical composition. *Atmospheric Chemistry and Physics*, *18*(17), 13,155–13,171. https://doi.org/10.5194/acp-18-13155-2018

Tham, Y. J., Wang, Z., Li, Q., Yun, H., Wang, W., Wang, X., et al. (2016). Significant concentrations of nitryl chloride sustained in the morning: Investigations of the causes and impacts on ozone production in a polluted region of northern China. *Atmospheric Chemistry and Physics*, *16*, 14,959–14,977.

Tham, Y. J., Yan, C., Xue, L., Zha, Q., Wang, X., & Wang, T. (2014). Presence of high nitryl chloride in Asian coastal environment and its impact on atmospheric photochemistry. *Chinese Science Bulletin*, *59*(4), 356–359.

Tie, X., Madronich, S., Walters, S., Zhang, R., Rasch, P., & Collins, W. (2003). Effect of clouds on photolysis and oxidants in the troposphere. *Journal of Geophysical Research*, *108*(D20), 4642. https://doi.org/10.1029/2003JD003659

Verstraeten, W. W., Neu, J. L., Williams, J. E., Bowman, K. W., Worden, J. R., & Boersma, K. F. (2015). Rapid increases in tropospheric ozone production and export from China. *Nature Geoscience*, *8*(9), 690.

Wang, T., Tham, Y. J., Xue, L., Li, Q., Zha, Q., Wang, Z., et al. (2016). Observations of nitryl chloride and modeling its source and effect on ozone in the planetary boundary layer of southern China. *Journal of Geophysical Research: Atmospheres*, *121*, 2476–2489. https://doi.org/10.1002/2015JD024556

Wang, T., Xue, L., Brimblecombe, P., Lam, Y. F., Li, L., & Zhang, L. (2017). Ozone pollution in China: A review of concentrations, meteorological influences, chemical precursors, and effects. *Science of the Total Environment*, *575*, 1582–1596. https://doi.org/10.1016/j.scitotenv.2016.10.081

Wang, X., Jacob, D. J., Eastham, S. D., Sulprizio, M. P., Zhu, L., Chen, Q., et al. (2019). The role of chlorine in global tropospheric chemistry. *Atmospheric Chemistry and Physics*, *19*(6), 3981–4003.

Wang, X., Wang, H., Xue, L., Wang, T., Wang, L., Gu, R., et al. (2017). Observations of N2O5 and ClNO2 at a polluted urban surface site in North China: High N2O5 uptake coefficients and low ClNO2 product yields. *Atmospheric Environment*, *156*, 125–134.

Wang, Z., Wang, W. H., Tham, Y. J., Li, Q. Y., Wang, H., Wen, L., et al. (2017). Fast heterogeneous N2O5 uptake and ClNO2 production in power plant and industrial plumes observed in the nocturnal residual layer over the North China plain. *Atmospheric Chemistry and Physics*, *17*, 12,361–12,378.

Wiedinmyer, C., Akagi, S. K., Yokelson, R. J., Emmons, L. K., Al-Saadi, J. A., Orlando, J. J., & Soja, A. J. (2011). The fire INventory from NCAR (FINN): A high resolution global model to estimate the emissions from open burning. *Geoscientific Model Development*, *4*(3), 625.

Xue, L. K., Saunders, S. M., Wang, T., Gao, R., Wang, X. F., Zhang, Q. Z., & Wang, W. X. (2015). Development of a chlorine chemistry module for the master chemical mechanism. *Geoscientific Model Development*, *8*, 3151–3162.

Yang, X., Wang, T., Xia, M., Gao, X., Li, Q., Zhang, N., et al. (2018). Abundance and origin of fine particulate chloride in continental China. *Science of the Total Environment*, *624*, 1041–1051. https://doi.org/10.1016/j.scitotenv.2017.12.205

Young, P. J., Archibald, A. T., Bowman, K. W., Lamarque, J. F., Naik, V., Stevenson, D. S., et al. (2013). Pre-industrial to end 21st century projections of tropospheric ozone from the atmospheric chemistry and climate model Intercomparison project (ACCMIP). *Atmospheric Chemistry and Physics*, *13*(4), 2063–2090. https://doi.org/10.5194/acp-13-2063-2013

Yun, H., Wang, W., Wang, T., Xia, M., Yu, C., Wang, Z., et al. (2018). Nitrate formation from heterogeneous uptake of dinitrogen pentoxide during a severe winter haze in southern China. *Atmospheric Chemistry and Physics*, *18*(23), 17,515–17,527. https://doi.org/10.5194/acp-18-17515-2018

Zaveri, R. A., Easter, R. C., Fast, J. D., & Peters, L. K. (2008). Model for simulating aerosol interactions and chemistry (MOSAIC). *Journal of Geophysical Research*, *113*(D13), D13204. https://doi.org/10.1029/2007JD008782

Zhang, L., Li, Q. Y., Wang, T., Ahmadov, R., Zhang, Q., Li, M., & Lv, M. Y. (2017). Combined impacts of nitrous acid and nitryl chloride on lower-tropospheric ozone: New module development in WRF-Chem and application to China. *Atmospheric Chemistry and Physics*, *17*(16), 9733–9750.

Zheng, B., Tong, D., Li, M., Liu, F., Hong, C., Geng, G., et al. (2018). Trends in China's anthropogenic emissions since 2010 as the consequence of clean air actions. *Atmospheric Chemistry and Physics*, *18*(19), 14,095–14,111. https://doi.org/10.5194/acp-18-14095-2018

Zhou, W., Zhao, J., Ouyang, B., Mehra, A., Xu, W., Wang, Y., et al. (2018). Production of N 2 O 5 and ClNO 2 in summer in urban Beijing, China. *Atmospheric Chemistry and Physics*, *18*(16), 11,581–11,597. https://doi.org/10.5194/acp-18-11581-2018